Role of OAS gene family in COVID-19 induced heart failure

LiJuan Gao[1], * ZhongMei[1], Xuan Shang[1], RuiRui Yang[1], Min Yan[1], and Ji-Min Cao[1]

[1]Laboratory of Cell Physiology INSERM U1003

October 5, 2022

Abstract

COVID-19 can lead to heart failure (HF) and even cardiac death. The 2',5'-oligoadenylate synthetase (OAS) gene family is associated with the antiviral immune responses of COVID-19. While the potential association of OAS family with cardiac injury and failure in COVID-19 has not been determined. Hence, in our study, the expression levels and biological functions of OAS gene family in SARS-CoV-2 infected cardiomyocytes dataset (GSE150392) and HF dataset (GSE120852) were determined by comprehensive bioinformatic analysis and experimental validation. miRNAs targeting OAS gene family were explored from Targetscan and HF miRNA database. The potential OAS gene family-regulatory chemicals or ingredients were predicted using Comparative Toxicogenomics Database (CTD) and SymMap database. Results showed that OAS genes were highly expressed in both SARS-CoV-2 infected cardiomyocytes and failing hearts. The differentially expression genes (DEGs) in two datasets were enriched in cardiovascular disease and COVID-19 related pathways, respectively. The miRNAs-target analysis indicated that 10 miRNAs increase OAS genes expression. A variety of chemicals or ingredients were predicted regulating the expression of OAS gene family, especially estradiol. In conclusion, OAS gene family is an important mediator of HF in COVID-19 and may serve as a potential therapeutic target for cardiac injury and HF in COVID-19.

1 INTRODUCTION

Coronavirus disease 2019 (COVID-19), caused by severe acute respiratory syndrome coronavirus 2 (SARS-CoV-2) infection (Wu F. et al., 2020), is a highly transmissible and pathogenic coronavirus emerged in late 2019 and has greatly threatened human health and public safety worldwide (Lu R. et al., 2020). Patients with COVID-19 exhibit a variety of symptoms, such as cough, fever, chest discomfort, and even respiratory distress syndrome in severe cases (Habas et al., 2020). Those with comorbidities, older age and male sex tend to suffer from severe COVID-19 after infection (Hu, Guo, Zhou, & Shi, 2021; Wu C. et al., 2020). In addition to causing severe respiratory illness, COVID-19 can also damage multiple organs especially the heart, causing myocardial injury and HF (Khan et al., 2020; Boukhris et al., 2020). HF is the fourth most frequent complication of COVID-19 (Zhou F. et al., 2020), and is also the final outcome of most cardiovascular diseases. The mortality rate of HF is extremely high (McMurray & Pfeffer, 2005). Therefore, it is necessary to investigate the regulatory mechanisms of HF in COVID-19 in order to better control the worse cardiac consequences of this infectious disease.

In human genome, OAS gene family includes OAS1, OAS2, OAS3, and OASL (Gao et al., 2022; Hornung, Hartmann, Ablasser, & Hopfner, 2014). As an important immune regulator (Boroujeni et al., 2021), OAS gene family participates in antiviral biological process and innate immune. Upon virus infection, OAS genes catalyze ATP into 2',5'-linked oligomers of adenosine in the presence of double-stranded (ds) RNA. These oligomers then activate RNaseL (Rebouillat & Hovanessian, 1999; Rebouillat, Hovnanian, David, Hovanessian, & Williams, 2000). OAS proteins act as a sensor of dsRNA and block viral replication by activating RNaseL (Schwartz S. L. & Conn G. L., 2019; Eskildsen, Hartmann, Kjeldgaard, & Justesen, 2002). In this process, NOD-like proteins can interact with the OAS family to enhance the activity of RNase L. The degraded RNA activates retinoic acid-inducible gene-I (RIG-1) (Schwartz Samantha L. & Conn Graeme L., 2019; Chakrabarti, Jha, & Silverman, 2011). RIG-1 amplify production of IFN-α/β and

activate NF-ϰB to produce inflammatory factors, leading to cell apoptosis (Ronni et al., 1997). In addition, the JAK-STAT pathway and IFN regulatory factor (IRF) family are involved in the regulation of this process (Samuel, 2001). However, it is unknown whether the OAS gene family actually plays a beneficial or harmful role in SARS-CoV-2-infected cardiomyocytes and COVID-19-induced cardiac injury and failure, because activations of antiviral genes do not necessarily produce a beneficial effect on the viral diseases such as COVID-19.

In the present study, we speculated that OAS gene family is an effective mediator for COVID-19 to worsen the cardiac function and cause HF. Numerous studies have found that untimely or overreacted antiviral responses may cause imbalance of the immune system, leading to inflammatory response or cytokine storm (Pasrija & Naime, 2021). SARS-CoV-2 infects the respiratory cells and other cells including the cardiomyocytes, causes host cell apoptotic death by inducing inflammation and even cytokine storm (Li et al., 2021; Guzik et al., 2020), thus may worsen the cardiac function and cause HF, one of the most common outcomes of COVID-19. Here, using extensive bioinformatic analyses and experimental validation, we found that the expressions of OAS genes were significantly upregulated in both the SARS-CoV-2-infected cardiomyocytes and in the failing hearts of COVID-19-free cases. These findings support our speculation and suggest that OAS gene family promotes the development of HF in COVID-19. Targeting OAS genes may be a potential therapeutic approach in treating COVID-19 associated HF.

2 MATERIALS AND METHODS

2.1 Data download and processing

The original gene expression profiles of GSE150392, GSE120852, GSE147507, GSE 179850 and GSE104150 were download from the National Center of Biotechnology Information - Gene Expression Omnibus (NCBI-GEO) database (https://www.ncbi.nlm.nih.gov/geo/), the largest, free and open accessing public gene expression database presently in the world.

GSE150392 is a dataset of mRNA expression in SARS-CoV-2 infected cardiomyocytes, including three groups of SARS-CoV-2 infected hiPSC-cardiomyocytes and three groups of hiPSC-cardiomyocytes with mock. The detailed information of GSE150392 dataset is shown in Table 1.

GSE120852 is a mRNA expression dataset of HF (COVID-19 free), including 5 non-failing (NF) left ventricles (LV), 5 NF right ventricles (RV), 5 LV tissues from subjects of LV failure, 5 RV tissues from LV failure, 5 LV tissues from biventricular failure (Bi-HF), and 5 RV tissues from Bi-HF. In the condition of LV failure, the mRNA expression profiles of LV and the RV were extracted and compared with the corresponding normal ventricular tissues (non-failing ventricles) to obtain the differential gene 1 (diff-1) and gene 2 (diff-2). In the condition of biventricular failure, the mRNA expression profiles of LV and the RV were derived and compared with that of the corresponding normal ventricular tissues to obtain the differential gene 3 (diff-3) and gene 4 (diff-4). The detailed information of GSE120852 dataset is shown in Table 2.

GSE147507 and GSE179850 are mRNA expression databsets related with COVID-19. In GSE147507, we chose three groups of human lung epithelial (NHBE) cells treated with mock and three groups of NHBE cells treated with SARS-CoV-2, the detailed information is showed in Table 3. In GSE179850, there are 16 groups of healthy controls and 31 groups of COVID-19 patients blood samples, details are displayed in Table 4.

GSE104150 is a microRNA (miRNA) expression dataset of HF, including seven groups of blood samples from healthy controls and nine groups of blood samples from HF subjects. The detailed information of GSE104150 dataset is shown in Table 5.

2.2 Analyses of Gene Ontology (GO) and Kyoto Encyclopedia of Genes and Genomes (KEGG) pathways enrichment

GO and KEGG pathways of DEGs were analyzed using Metascape. Metascape (Zhou et al., 2019) (http://metascape.org) is a public online database, it is designed to provide a comprehensive gene list

annotation and analysis resource. GO is a gene function classification system to describe gene property. In the GO enrichment analysis, three aspects were analyzed, including biological processes (BP), cellular components (CC), and molecular functions (MF). KEGG pathway was used to analyze gene function, genomic information, and target relationship of pathways. $P < 0.01$ was chosen as the cut-off criteria.

2.3 Creation ofmouse heart failure model

Eight-week-old male C57BL/6 mice (22-25 g) were purchased from Sibeifu Co., (Beijing). All mice were maintained under specific-pathogen-free (SPF) conditions. HF in the mice were induced by transverse aortic constriction (TAC) for 8 weeks. TAC surgery was conducted as reported by Tavakoli et al. (Tavakoli, Nemska, Jamshidi, Gassmann, & Frossard, 2017) and Wu et al. (Wu L. F. et al., 2022). Pressure gradients between the proximal and distal sites of TAC were determined by doppler echocardiography. Heart weight/body weight (HW/BW) ratio, ejection fraction (EF), fractional shortening (FS), left ventricular posterior wall thickness at end diastole (LVPWd), and left ventricular posterior wall thickness at systole (LVPWs) were calculated.

2.4 culture and treatment

H9C2 cells (a rat myocardial cell line) were purchased from Shanghai Institutes for Biological Sciences, Chinese Academy of Sciences (Shanghai, China), and cultured in 6-well plates using DMEM with 10% fetal bovine serum and 1% penicillin/streptomycin at 37 in a humidified environment containing 5% CO_2. Cells were cultured in serum-free DMEM medium for 12 h, then were challenged with angiotensin II (Ang II) for 48 h to induce cardiomyocyte hypertrophic injury. Cells were harvested for quantitative real-time PCR (qPCR).

2.5 RNA isolation and qPCR

Total mRNA was extracted from mice failing heart tissues and H9C2 cells using TRIzol (Invitrogen, Carlsbad, CA), then was reverse-transcribed into cDNA according to the instructions of TaKaRa PrimeScript RT reagent Kit with gDNA Eraser (TaKaRa, Osaka, Japan), according to the manufacturer's instruction. PCR amplifications were quantified according to the instructions of TaKaRa TB Green Premix Ex Taq II (TaKaRa, Osaka, Japan). The primer sequences for qPCR were designed by Sangon Biotech Co., Ltd (Shanghai, China). The expression data were normalized to the reference glyceraldehyde-3-phosphate dehydrogenase (GAPDH) and the mRNA levels were calculated using the $2^{-[?][?]Ct}$ method. Primer sequences for qPCR are shown in Table S1.

2.6 Analysis of differentially expressed genes (DEGs)

The "limma" package in the R language was used to analyze the data downloaded from NCBI-GEO. $P < 0.05$ and $|logFC| > 1$ were chosen as the cut-off criteria in the analyses of GSE150392 and GSE104150; $P < 0.05$ and $|logFC| > 0.8$ were set as the cut-off criteria in GSE120852. The common DEGs in GSE120852 were generated and visualized using FunRich software (version 3.1.3.).

2.7 Analysis of DEGs interactions and screening of hub genes

The protein-protein interaction (PPI) network of DEGs were determined using STRING (Szklarczyk et al., 2014) (version 11.5, https://string-db.org/). STRING is an online database for searching protein-protein interactions including direct physical interactions and indirect functional correlations between proteins. In the PPI analysis, the minimally required interaction score was set as medium confident 0.4. Then, results were used to screen hub genes using CytoHubba in Cytoscape (version 3.9.0.). CytoHubba (Chin et al., 2014) is a plugin in Cytoscape, it provides 12 topological analysis methods which can be used to explore important nodes in biological networks. We used Density of Maximum Neighborhood Component (DMNC), one of the 12 topological analysis methods, to search the top 30 hub genes.

2.8 Analysis of miRNAstargeting the OAS gene family

The microRNAs (miRNAs) are short non-coding RNA molecules with 19 to 25 nucleotides in size and have the functions of degrading or blocking target mRNAs at the post-transcriptional level (Lu T. X. & Rothenberg, 2018). Targetscan (Györffy et al., 2010) (http://www.targetscan.org/vert_72/) was used to identify the upstream miRNAs of OAS gene family.

2.9 Prediction of chemicals andingredients interacting with OAS gene family

Comparative Toxicogenomics Database (CTD) and SymMap database were used to analyze the chemicals or drugs which interact with the OAS gene family. CTD (Davis et al., 2021) (http://ctdbase.org/) is a powerful public database which integrates large amounts of data among chemicals, genes, functional phenotypes and diseases. It provides information on the associations of chemical-gene/protein, chemical-disease, and gene-disease, and thus helps to predict mechanistic hypotheses about the influence of environment on disease. In the CTD database, we chose chemicals with "interaction" > 3 as the cut-off criteria to perform further analysis. SymMap (Wu Y. et al., 2019) database (http://www.symmap.org/) is an integrative database of Traditional Chinese Medicine (TCM) enhanced by symptom mapping. It contains six components, including herbs, TCM symptoms, modern medicine (MM) symptoms, ingredients, targets (or genes) and disease. Target function was used to analyze the ingredients that interact with the OAS gene family.

2.10 Docking analysis of affinity between

chemicals/ingredients and OAS gene family

Molecular docking approach was used to identify the affinities of chemicals/ingredients with OAS1, OAS2, OAS3, and OASL. The structures of the small molecules from PubChem database (https://pubchem.ncbi.nlm.nih.gov/) were downloaded, and Chem3D software was used to minimize the ligand molecular energy. The 3D structures of OAS genes were obtained from PDB database (https://www1.rcsb.org/) or UniProt database (https://www.uniprot.org/). AutoDockTools 1.5.6 software was used to find out the active pockets. Vina script was run to calculate the molecular binding energy, Vina [?] -7.0 kcal*mol^{-1}indicated strong binding of "ligand" with "receptor". PyMOL software was used to display the results.

2.11 Statistical analysis

GraphPad Prism 5.0 were used to performed statistical analysis. Data were presented as mean +- standard deviation (SD). Two-tail t-test was used for comparison of two groups. Statistical significance was set at $P < 0.05$.

3 RESULTS

3.1 DEGs and hub genesderived from the GSE150392 dataset

In GSE150392 (mRNA expression dataset of SARS-CoV-2 infected cardiomyocytes), a total of 1,448 DEGs were screened out. Among them, 745 DEGs were up-expressed and 703 DEGs were down-expressed. Notably, OAS1, OAS2, OAS3, and OASL were all up-expressed in the cardiomyocytes with SARS-CoV-2 infection (Figures 1A, B; Table S2), and their logFCs were 6.94, 7.13, 5.83, and 5.49, respectively (Figure 1C).

The protein-protein interactions among the DEGs were analyzed using STRING online database and results were presented using cytoscape (Figure 1D). In this analysis, the algorithms of DMNC in the plugin cytoHubba was used to calculate the top 30 hub genes. OAS1, OAS2, OAS3, and OASL were ranked 14, 13, 9, and 28 among the top 30 hub genes, respectively (Figure 1E).

3.2 DEGs and hub genes derived from the GSE120852 dataset

In GSE120852 (mRNA expression dataset of HF), four groups were included and their intersection genes (common DEGs) were selected to perform further analysis. Diff-1 indicated the comparison result of LV heart failure (LV-HF) vs. non-failing LV (LV-NF). As a result, 849 DEGs were screened out, 507 were up-expressed and 342 DEGs were down-expressed. Diff-2 was obtained from RV which reflected the RV mRNA difference between LV-HF and LV-NF. In the Diff-2 analysis, 1,128 DEGs were screened out, and

among them, 638 were up-expressed and 490 DEGs were down-expressed. Diff-3 was obtained from LV by comparing biventricular heart failure (Bi-HF) and non-failing (NF) hearts. Total 973 DEGs were screened out, in which 614 were up-expressed and 359 DEGs were down-expressed. Diff-4 was gained from RV by comparing Bi-HF and NF hearts, total 1,175 DEGs were screened out, 673 were up-expressed and 502 DEGs were down-expressed (Figures 2A, B; Table S3). Total 239 common DEGs were found in the above four groups of DEGs, and 169 were up-expressed and 70 were down-expressed (Figure 2C). Of note, OAS1, OAS2, OAS3 and OASL were all highly expressed in HF. In diff-1, the logFCs of OAS1, OAS2, OAS3, and OASL were 1.04, 0.81, 0.98, and 1.03, respectively. In diff-2, the logFCs of OAS1, OAS2, OAS3 and OASL were 1.23, 0.97, 1.22, and 1.53, respectively. In diff-3, the logFCs of OAS1, OAS2, OAS3 and OASL were 1.35, 1.03, 0.93, and 1.57, respectively. In diff-4, the logFCs of OAS1, OAS2, OAS3 and OASL were 1.26, 1.21, 1.37 and 1.94, respectively. (Figure 2D).

SRTING online software was used to explore the relationships among the 239 common DEGs, and results were shown via cytoscape (Figure 2E). The algorithm of DMNC in plugin cytoHubba was used to calculate the top 30 hub genes. To our speculation, OAS1, OAS2, OAS3, and OASL were all among the top 30 hub genes, and they were ranked 15, 6, 6, and 2, respectively (Figure 2F).

3.3 Experimental validation of high mRNA expressions of OAS genes

To verify the expression of OAS genes shown in Figures 1 and 2, we further analyzed the GSE147507 dataset (SARS-CoV-2 infected NHBE) and the GSE179850 dataset (blood sample of COVID-19 patients) to evaluate the expression of OAS gene family in alternative tissues of COVID-19 patients. Results demonstrated that OAS1, OAS2, OAS3, and OASL were all highly expressed in SARS-CoV-2 infected NHBE (Figure 3 A) (OAS 1-3, $P < 0.01$) and in the blood leucocytes of COVID-19 patients (Figure 3B) (all $P < 0.001$). In addition, the qPCR results of 8-week TAC mice and Ang II-stimulated H9C2 cells showed that the mRNA levels of atrial natriuretic peptide (ANP), brain natriuretic peptide (BNP), and myosin heavy chain β (β-MHC) were all significantly increased in the cardiac tissues of TAC mice (Figure 4A, B) and Ang II-challenged H9C2 cells (Figure 4C, D) , and the mRNA levels of OAS1, OAS2, OAS3, and OASL were also significantly elevated in the failing hearts of TAC mice (Figures 4B) and Ang II-treated H9C2 cells (Figures 4D). These results indicate a consistence between the bioinformatic analysis and the experimental validation.

3.4 GO and KEGG pathway analyses revealing the intersecting signaling between COVID-19 and HF

The biological function enrichment analyses of DEGs in GSE150392 and GSE120852 datasets were performed using Metascape.

Results of GO analysis from GSE150392 are shown in Figure 5A and Table S4. The DEGs of GSE150392 were significantly enriched in GO:0048018 (MF: receptor ligand activity), GO:0030017 (CC: sarcomere), GO:0071345 (BP: cellular response to cytokine stimulus), GO:0003013 (BP: circulatory system process), GO:0044057 (BP: regulation of system process), GO:0030155(BP: regulation of cell adhesion), GO:0001819(BP: positive regulation of cytokine production), GO:0009615 (BP: response to virus), GO:0010817 (BP: regulation of hormone levels), GO:0044706 (BP: multi-multicellular organism process), GO:0043408 (BP: regulation of MAPK cascade), GO:0006936 (BP: muscle contraction), GO:0043269 (BP: regulation of ion transport), GO:0061061(BP: muscle structure development), GO:0007167 (BP: enzyme-linked receptor protein signaling pathway), GO:0050900 (BP: leukocyte migration), GO:0032649 (BP: regulation of interferon-gamma production), GO:0010942(BP: positive regulation of cell death), GO:0009725(BP: response to hormone), and GO:0048511(BP: rhythmic process). Results of KEGG pathway analysis from GSE150392 were displayed in Figure 5B and Table S5. The DEGs of GSE150392 were significantly enriched in hsa04668 (TNF signaling pathway), hsa04060 (cytokine-cytokine receptor interaction), hsa04260 (Cardiac muscle contraction), hsa05164 (influenza A), hsa05202 (transcriptional misregulation in cancer), hsa05143 (African trypanosomiasis), hsa04010 (MAPK signaling pathway), hsa04080 (neuroactive ligand-receptor interaction), hsa04020 (calcium signaling pathway), hsa05415 (Diabetic cardiomyopathy), hsa04913 (ovarian steroidogenesis), hsa04210 (apoptosis), hsa04750 (inflammatory mediator regulation of TRP chan-

nels), hsa05203 (viral carcinogenesis), hsa00350 (tyrosine metabolism), hsa04670 (leukocyte transendothelial migration), hsa04727 (GABAergic synapse), hsa04024 (cAMP signaling pathway), hsa04630 (JAK-STAT signaling pathway), and hsa04713 (circadian entrainment).

Results of GO analysis from GSE120852 were shown in Figure 6A and Table S6. The DEGs of this analysis included GO:0031012 (CC: extracellular matrix), GO:0030155 (BP: regulation of cell adhesion), GO:0006935 (BP: chemotaxis), GO:0098552 (CC: side of membrane), GO:0098609 (BP: cell-cell adhesion), GO:0050900 (BP: leukocyte migration), GO:0005539 (MF: glycosaminoglycan binding), GO:0045321 (BP: leukocyte activation), GO:0005518 (MF: collagen binding), GO:0002685 (BP: regulation of leukocyte migration), GO:0002252 (BP: immune effector process), GO:0005178 (MF: integrin binding), GO:0005604 (CC: basement membrane), GO:0002683 (BP: negative regulation of immune system process), GO:0050727 (BP: regulation of inflammatory response), GO:0048525 (BP: negative regulation of viral process), GO:0032103 (BP: positive regulation of response to external stimulus), GO:0019221 (BP: cytokine-mediated signaling pathway), GO:0030934 (CC: anchoring collagen complex), and GO:0046886 (BP: positive regulation of hormone biosynthetic process). Results of KEGG pathway analysis from GSE120852 were displayed in Figure 6B and Table S7. The DEGs of this analysis included hsa05164 (influenza A), hsa04060 (cytokine-cytokine receptor interaction), hsa04062 (chemokine signaling pathway), hsa04974 (protein digestion and absorption), hsa04670 (leukocyte transendothelial migration), hsa05171 (coronavirus disease-COVID-19), hsa05340 (primary immunodeficiency), hsa04210 (apoptosis), hsa04064 (NF-kappa B signaling pathway), hsa04929 (GnRH secretion), hsa00260 (glycine, serine and threonine metabolism), hsa04380 (osteoclast differentiation), hsa04926 (relaxin signaling pathway), hsa00480 (glutathione metabolism), hsa03250 (viral life cycle-HIV-1), hsa05221 (acute myeloid leukemia), hsa05120 (epithelial cell signaling in helicobacter pylori infection), hsa04512 (ECM-receptor interaction), and hsa04350 (TGF-beta signaling pathway).

Results of GSE150392 analysis, including GO:0003013 (circulatory system process) and hsa04260 (cardiac muscle contraction), were related to cardiac function in SARS-CoV-2 infected cardiomyocytes. Some results from GSE120852, such as GO:0050727 (regulation of inflammatory response) and hsa05171 (COVID-19), were also related to COVID-19. In addition, some results, including GO:0030155 (BP: regulation of cell adhesion), GO:0006935 (BP: chemotaxis), GO:0050900 (BP: leukocyte migration), hsa05164 (Influenza A), hsa04060 (Cytokine-cytokine receptor interaction), hsa04670 (leukocyte transendothelial migration), and hsa04210 (apoptosis), were common results of GSE150392 and GSE120852, suggesting that the processes of HF and COVID-19 employ the same biological pathways to some extents.

3.5 The miRNAs regulating the expression of OAS gene family

To explore the regulatory mechanism of OAS gene family expression, we analyzed the miRNAs derived from GSE104150 (miRNA expression dataset of HF) and took intersection with the predicting results from Targetscan. Total 88 different miRNAs were obtained from GSE104150, and among them, 22 miRNAs were upregulated and 44 miRNAs were downregulated (Figure 7A, B; Table S8). From the intersection of Targetscan and GSE104150, we found that 6 miRNAs regulated OAS1, including hsa-miR-1225-5p, hsa-miR-1229-5p, hsa-miR-15a-3p, hsa-miR-4270, hsa-miR-6751-3p, and hsa-miR-7106-5p. There were 33 miRNAs that regulated OAS2, including hsa-miR-1225-5p, hsa-miR-1229-5p, hsa-miR-1275, hsa-miR-181a-5p, hsa-miR-197-5p, hsa-miR-2392, hsa-miR-23a-5p, hsa-miR-26b-5p, hsa-miR-3149, hsa-miR-4433a-3p, hsa-miR-4459, hsa-miR-4484, hsa-miR-4499, hsa-miR-4632-5p, hsa-miR-4721, hsa-miR-4769-3p, hsa-miR-5196-5p, hsa-miR-548aq-5p, hsa-miR-548d-5p, hsa-miR-576-5p, hsa-miR-5787, hsa-miR-580-3p, hsa-miR-6124, hsa-miR-671-5p, hsa-miR-6751-3p, hsa-miR-6752-5p, hsa-miR-6756-5p, hsa-miR-6785-5p, hsa-miR-6812-5p, hsa-miR-6850-5p, hsa-miR-6893-5p, hsa-miR-7106-5p, hsa-miR-7641. There were 4 miRNAs that regulated OAS3, they were hsa-miR-1273g-3p, hsa-miR-197-3p, hsa-miR-23a-5p, and hsa-miR-3149. There were 5 miRNAs regulated OASL, including hsa-miR-6812-5p, hsa-miR-5787, hsa-miR-671-5p, hsa-miR-1273g-3p, hsa-miR-186-3p (Figure 7C). These intersecting miRNAs were shown in Figure 7D and Table S9.

Among these intersecting miRNAs, 10 miRNAs, including hsa-miR-15a-3p, hsa-miR-23a-5p, hsa-miR-26b-5p, hsa-miR-186-3p, hsa-miR-4433a-3p, hsa-miR-548aq-5p, hsa-miR-548d-5p, hsa-miR-576-5p, hsa-miR-580-3p, and hsa-miR-6850-5p, were down-expressed, this may be the reason for the high expression of OAS gene

family in HF.

3.6 Predicted chemicals andingredientsinteracting with OAS gene family

CTD and SymMap databases were used to predict the chemicals and ingredients that may interact with the OAS genes. CTD results showed that 12, 14, 10, and 6 chemicals interacted with OAS1, OAS2, OAS3, and OASL, respectively. Notably, estradiol and tetrachlorodibenzodioxin were found the common chemicals regulating the four OAS genes (Figure 8A). SymMap results showed that 4, 3, 5, and 4 ingredients acted on OAS1, OAS2, OAS3, and OASL, respectively. Among them, 17-β-estradiol, hydrargyrum and saccharose were the common chemicals or ingredients that regulated the OAS gene family (Figure 8B). The 17-β-estradiol, also named estradiol (Dubey & Jackson, 2001), were commonly recommended by CTD and SymMap database.

3.7 Results ofdocking analysis

The 3D structure of OAS1 was obtained from PDB database (PDB ID: 4IG8), and the 3D structures of OAS2, OAS3, and OASL were downloaded from UniProt database. The binding energies of 17-β-estradiol with OAS1, OAS2, OAS3, and OASL were -7.1 kcal·mol^{-1}, -7.6 kcal*mol^{-1}, -8.4 kcal*mol^{-1}, and -8.7 kcal*mol^{-1}, respectively, suggesting that the bonding between 17-β-estradiol and the four "receptors" (OAS proteins) were strong. From the results of ligand-receptor protein interaction, we found that 17-β-estradiol could form hydrophilic binding with SER63, GLN229, and THR19, and had hydrophobic interactions with the amino acid residues ASP77, GLY62, GLN194, LEU150, and THR188 of OAS1 (Figure 9A). In addition, 17-β-estradiol exhibited hydrophilic force with LEU340 and LYS556, while had hydrophobic force with PHE341, TRP663, GLU552, PRO339, LEU340, GLN235, GLU659, and MET266, of OAS2 (Figure 9B). The 17-β-estradiol also had hydrophilic effects on the ARG65 of OAS3 while had hydrophobic effects on ALA182, TRP303, GLY61, ASP74, SER145, GLU76, VAL125, VAL147, and ALA128 of OAS3 (Figure 9C). Furthermore, 17-β-estradiol showed hydrophilic bonding with ASN72, GLU237 and VAL132 but hydrophobic interaction with TYR234, GLY68, GLU83, VAL67, CYS188, SER192, GLN185 and VAL199 of OASL (Figure 9D). These forces made 17-β-estradiol stably binding to the pockets of the four OAS proteins.

4 DISCUSSION

The highlight of this study was the discovery of an important role of OAS gene family in the process of COVID-19 induced HF. HF is one of the major adverse consequences of COVID-19 (Zhou Fei et al., 2020). The fact that OAS genes were highly expressed in both SARS-CoV-2-infected cardiomyocytes and human HF tissues provides us a reason to believe that some similar signaling molecules may mediate the developments of COVID-19 and HF. Or in other words, there may be some similar or common molecular mechanisms in the two diseases, and OAS genes may be the common genetic factors. Based on the present bioinformatics analysis (shown in Figure 1 and Figure 3) and previous reports, OAS genes are highly expressed in SARS-CoV-2 infected cardiomyocytes and COVID-19 patients (Baranova, Cao, & Zhang, 2021; Pairo-Castineira et al., 2021; Shaath, Vishnubalaji, Elkord, & Alajez, 2020; Kotsev et al., 2021), and our qPCR experiments further verified the high expressions of OAS genes in the myocardium of COVID-19-free HF cases (shown in Figure 2 and Figures 4). Previous studies have reported that OAS cluster variants are associated with greater risk of severe COVID-19, and OAS gene family plays an important role in the innate antiviral mechanisms linking to SARS-CoV-2 infection (Pairo-Castineira et al., 2021; Kotsev et al., 2021; "Mapping the human genetic architecture of COVID-19," 2021; Steffen et al., 2022). These findings may be associated with the immune dysregulation and cytokine storm leading to HF in COVID-19 patients (Azevedo et al., 2021; Tajbakhsh et al., 2021). During the cytokine storm, a large number of inflammatory factors are produced, such as TNF-α, IL-1, IL-6, and IFN-γ, leading to severe inflammation, multi-organ failure and even death. Several previous studies have reported that cytokine storm can occur in COVID-19 patients, and the level of pro-inflammatory factors is positively correlated with disease severity (Chen et al., 2020; (Huang et al., 2020). This may be a crucial reason for developing HF in COVID-19 cases.

To corelate OAS gene family with COVID-19 associated HF, it is worthy to mention the important roles of IFN and IFN-stimulated genes (ISGs) in the endogenous anti-virus processes. OAS gene family is closely

related to the induction of IFN (Samuel, 2001). In COVID-19 patients, SARS-CoV-2 strongly triggers the expressions of many ISGs and activates immune cells. ISGs have immunopathogenic potentials, including overexpression of inflammatory genes. In some COVID-19 cases, the level of IFN-I is low at the early stage, leading to excessive viral proliferation; when the IFN-I reaches a high level at the advanced stage, it may be too late to be rescued. Massive viral replication and early immune escape result in hyperactivation of pro-inflammatory responses (van der Made et al., 2020; Zhou Z. et al., 2020; Ramasamy & Subbian, 2021). In severe COVID-19 cases, IFN-I response arouses an excessive inflammatory response by promoting TNF/IL-1β-driven inflammation leading to cytokine storm (Lee et al., 2020). As the critical members of innate immunity, OAS genes play important roles in immune responses and even the cytokine storm, this may one reason why COVID-19 can develop to HF. Zhang et al. (Zhang Cheng, Feng, Tam, Wang, & Feng, 2021) found a highly preserved transcriptional profile of IFN-I dependent genes for COVID-19 complementary diagnosis, and OAS genes were included in the profile. These evidences suggest the important role of OAS gene family in COVID-19. Adeghate et al. (Adeghate, Eid, & Singh, 2021) reported that SARS-CoV-2 invasion can damage the heart via the following mechanisms: 1) inflammatory cells infiltrate into the myocardium; 2) pro-inflammatory cytokines cause cardiomyocyte death; 3) viruses damage the endothelial cells coupled with micro-thrombosis; 4) hypoxia caused by respiratory failure indirectly contributes to HF. Among these mechanisms, OAS genes may take roles at least in some of them, for example, the immune responses.

COVID-19 is associated with many inflammation-related signaling pathways, such as interleukin-6/Janus kinase/STAT (IL-6/JAK/STAT) pathway, interferon (IFN) cell signaling pathway, tumor necrosis factor-α/nuclear factor-kappa (TNFα/NF-κB) pathway, toll-like receptor (TLR) pathway, T-cell receptor (TCR) pathway, etc. (Choudhary, Sharma, & Silakari, 2021; Zhang C., Wu, Li, Zhao, & Wang, 2020; Ritchie & Singanayagam, 2020). Our study on COVID-19 dataset reveals that inflammation-related pathways, such as hsa04668 (TNF signaling pathway), hsa04210 (Apoptosis), and hsa04630 (JAK-STAT signaling pathway), are consistent with the above viewpoint. These signaling pathways also have important biological functions in HF (Feldman et al., 2000; Sabbah & Sharov, 1998; Booz, Day, & Baker, 2002). In addition, our results show that after cardiomyocytes being infected by SARS-CoV-2, some HF-associated biological pathways became prevalent, such as hsa04260 (cardiac muscle contraction) and hsa05415 (diabetic cardiomyopathy), which directly indicates the signaling by which COVID-19 causes HF. By analyzing the DEGs in HF dataset GSE120852, we found that some signaling pathways associated with the DEGs, such as GO:0002252 (BP: immune effector process), GO:0002683 (BP: negative regulation of immune system process), GO:0050727 (BP: regulation of inflammatory response), hsa05171 (coronavirus disease-COVID-19), hsa04210 (apoptosis), and hsa04064 (NF-kappa B signaling pathway), are COVID-19 or inflammation related pathways. Especially, the term hsa05171 (coronavirus disease-COVID-19) from the HF dataset fully illustrates the close relationship of COVID-19 with HF.

Currently, there is no specific and effective drug for COVID-19. Thus, development of this kind of drugs is in urgent need. Some antiviral drugs have the potential to treat COVID-19, such as remdesivir, lopinavir/ritonavir, interferon β-1a, and hydroxychloroquine/chloroquine (Atzrodt et al., 2020). In the present study, we predicted some potential chemicals or ingredients which regulate the expression of OAS genes by analyzing the CTD and SymMap databases (shown in Figure 8). Notably, we found that estradiol is one of them. Except for regulating the sexual system, estradiol plays an important role in anti-inflammation and suppression of virus-induced innate immune inflammatory response. High physiological concentration of estradiol can reduce the production of pro-inflammatory cytokines, such as IL-6, IL-1β, TNF-α, and CCL2, and prevent migration of monocytes and neutrophils into inflamed tissues. Therefore, under the influence of estradiol, immune dysregulation caused by cytokine storm in COVID-19 is ameliorated (Pinna, 2021; Mauvais-Jarvis, Klein, & Levin, 2020). Women generally show better immune responses to viruses than men, men are more susceptible to severe COVID-19 (Klein, Jedlicka, & Pekosz, 2010; Docherty et al., 2020). A study proposed that a combination of estradiol with vitamin D and quercetin can be used to relieve COVID-19 (Glinsky, 2020). Estradiol also has a certain protective effect on cardiovascular diseases (Shufelt, Pacheco, Tweet, & Miller, 2018; Hodis et al., 2016). Estradiol can rescue severe HF through the

classical estrogen receptor beta (ERβ), which is present in the heart (Iorga et al., 2018). Frump et al. (Frump et al., 2021) reported that estradiol can protect the function of right ventricle in pulmonary hypertension via BMPR2 and apelin. These evidences suggest the protective effect of estradiol on the heart, including the heart damage in COVID-19.

The study has some limitations. We were unable to obtain cardiac tissues from COVID-19 and HF patients to verify the expression and mechanism of OAS gene family in these diseases. These issues warrant future studies.

5 CONCLUSION

In conclusion, we found that OAS genes are highly expressed in SARS-CoV-2 infected cardiomyocytes, tissues of COVID-19 patients, and COVID-19-free human failing hearts. OAS gene family strongly links COVID-19 with HF. OAS genes can interact with the invaded SARS-CoV-2 and activates the OAS/RNaseL antiviral system to degrade the virus. The degraded small RNA molecules activate NF-kB inflammation-related pathways, produce inflammatory factors or even cytokine storms, lead to cell death, and ultimately cause HF. The detailed flow is shown in Figure 10.

AUTHOR CONTRIBUTIONS

L.-J.G. and J.-M.C. conceived and designed the study. L.-J.G., Z.-M.H., X.S., R.-R.Y., M.Y. performed experiments, analyzed data and prepared figures. L.-J.G., drafted manuscript. J.-M.C. revised manuscript. All authors reviewed the manuscript.

FUNDING

This study was supported by National Natural Science foundation of China (82170523), Key Medical Science and Technology Program of Shanxi Province (2020XM01), Shanxi “1331” Project Quality and Efficiency Improvement Plan (1331KFC), and Basic Research Program of Shanxi Province (202103021223238).

ACKNOWLEDGEMENTS

We thank the mentioned public databases for providing us the data and analytical tools.

DECLARATION OF INTERESTS

The authors declare no conflict of interest in this work.

REFERENCES

Adeghate, E. A., Eid, N., & Singh, J. (2021). Mechanisms of COVID-19-induced heart failure: a short review. Heart Fail Rev, 26(2), 363-369. doi:10.1007/s10741-020-10037-x

Atzrodt, C. L., Maknojia, I., McCarthy, R. D. P., Oldfield, T. M., Po, J., Ta, K. T. L., Stepp, H. E., & Clements, T. P. (2020). A Guide to COVID-19: a global pandemic caused by the novel coronavirus SARS-CoV-2. Febs j, 287(17), 3633-3650. doi:10.1111/febs.15375

Azevedo, R. B., Botelho, B. G., Hollanda, J. V. G., Ferreira, L. V. L., Junqueira de Andrade, L. Z., Oei, S., Mello, T. S., & Muxfeldt, E. S. (2021). Covid-19 and the cardiovascular system: a comprehensive review. J Hum Hypertens, 35(1), 4-11. doi:10.1038/s41371-020-0387-4

Baranova, A., Cao, H., & Zhang, F. (2021). Unraveling Risk Genes of COVID-19 by Multi-Omics Integrative Analyses. Frontiers in medicine, 8, 738687. doi:10.3389/fmed.2021.738687

Booz, G. W., Day, J. N., & Baker, K. M. (2002). Interplay between the cardiac renin angiotensin system and JAK-STAT signaling: role in cardiac hypertrophy, ischemia/reperfusion dysfunction, and heart failure. J Mol Cell Cardiol, 34(11), 1443-1453. doi:10.1006/jmcc.2002.2076

Boroujeni, M. E., Simani, L., Bluyssen, H. A. R., Samadikhah, H. R., Zamanlui Benisi, S., Hassani, S., Akbari Dilmaghani, N., Fathi, M., Vakili, K., Mahmoudiasl, G. R., Abbaszadeh, H. A., Hassani Moghaddam,

M., Abdollahifar, M. A., & Aliaghaei, A. (2021). Inflammatory Response Leads to Neuronal Death in Human Post-Mortem Cerebral Cortex in Patients with COVID-19. ACS Chem Neurosci, 12(12), 2143-2150. doi:10.1021/acschemneuro.1c00111

Boukhris, M., Hillani, A., Moroni, F., Annabi, M. S., Addad, F., Ribeiro, M. H., Mansour, S., Zhao, X., Ybarra, L. F., Abbate, A., Vilca, L. M., & Azzalini, L. (2020). Cardiovascular Implications of the COVID-19 Pandemic: A Global Perspective. Can J Cardiol, 36(7), 1068-1080. doi:10.1016/j.cjca.2020.05.018

Chakrabarti, A., Jha, B. K., & Silverman, R. H. (2011). New insights into the role of RNase L in innate immunity. J Interferon Cytokine Res, 31(1), 49-57. doi:10.1089/jir.2010.0120

Chen, N., Zhou, M., Dong, X., Qu, J., Gong, F., Han, Y., Qiu, Y., Wang, J., Liu, Y., Wei, Y., Xia, J., Yu, T., Zhang, X., & Zhang, L. (2020). Epidemiological and clinical characteristics of 99 cases of 2019 novel coronavirus pneumonia in Wuhan, China: a descriptive study. Lancet, 395(10223), 507-513. doi:10.1016/s0140-6736(20)30211-7

Chin, C. H., Chen, S. H., Wu, H. H., Ho, C. W., Ko, M. T., & Lin, C. Y. (2014). cytoHubba: identifying hub objects and sub-networks from complex interactome. BMC Syst Biol, 8 Suppl 4(Suppl 4), S11. doi:10.1186/1752-0509-8-s4-s11

Choudhary, S., Sharma, K., & Silakari, O. (2021). The interplay between inflammatory pathways and COVID-19: A critical review on pathogenesis and therapeutic options. Microb Pathog, 150, 104673. doi:10.1016/j.micpath.2020.104673

Davis, A. P., Grondin, C. J., Johnson, R. J., Sciaky, D., Wiegers, J., Wiegers, T. C., & Mattingly, C. J. (2021). Comparative Toxicogenomics Database (CTD): update 2021. Nucleic Acids Res, 49(D1), D1138-d1143. doi:10.1093/nar/gkaa891

Docherty, A. B., Harrison, E. M., Green, C. A., Hardwick, H. E., Pius, R., Norman, L., Holden, K. A., Read, J. M., Dondelinger, F., Carson, G., Merson, L., Lee, J., Plotkin, D., Sigfrid, L., Halpin, S., Jackson, C., Gamble, C., Horby, P. W., Nguyen-Van-Tam, J. S., Ho, A., Russell, C. D., Dunning, J., Openshaw, P. J., Baillie, J. K., & Semple, M. G. (2020). Features of 20 133 UK patients in hospital with covid-19 using the ISARIC WHO Clinical Characterisation Protocol: prospective observational cohort study. Bmj, 369, m1985. doi:10.1136/bmj.m1985

Dubey, R. K., & Jackson, E. K. (2001). Cardiovascular protective effects of 17beta-estradiol metabolites. J Appl Physiol (1985), 91(4), 1868-1883. doi:10.1152/jappl.2001.91.4.1868

Eskildsen, S., Hartmann, R., Kjeldgaard, N. O., & Justesen, J. (2002). Gene structure of the murine 2'-5'-oligoadenylate synthetase family. Cell Mol Life Sci, 59(7), 1212-1222. doi:10.1007/s00018-002-8499-2

Feldman, A. M., Combes, A., Wagner, D., Kadakomi, T., Kubota, T., Li, Y. Y., & McTiernan, C. (2000). The role of tumor necrosis factor in the pathophysiology of heart failure. J Am Coll Cardiol, 35(3), 537-544. doi:10.1016/s0735-1097(99)00600-2

Frump, A. L., Albrecht, M., Yakubov, B., Breuils-Bonnet, S., Nadeau, V., Tremblay, E., Potus, F., Omura, J., Cook, T., Fisher, A., Rodriguez, B., Brown, R. D., Stenmark, K. R., Rubinstein, C. D., Krentz, K., Tabima, D. M., Li, R., Sun, X., Chesler, N. C., Provencher, S., Bonnet, S., & Lahm, T. (2021). 17β-Estradiol and estrogen receptor α protect right ventricular function in pulmonary hypertension via BMPR2 and apelin. The Journal of clinical investigation, 131(6), e129433. doi:10.1172/JCI129433

Gao, L. J., Li, J. L., Yang, R. R., He, Z. M., Yan, M., Cao, X., & Cao, J. M. (2022). Biological Characterization and Clinical Value of OAS Gene Family in Pancreatic Cancer. Front Oncol, 12, 884334. doi:10.3389/fonc.2022.884334

Glinsky, G. V. (2020). Tripartite Combination of Candidate Pandemic Mitigation Agents: Vitamin D, Quercetin, and Estradiol Manifest Properties of Medicinal Agents for Targeted Mitigation of the COVID-19

Pandemic Defined by Genomics-Guided Tracing of SARS-CoV-2 Targets in Human Cells. Biomedicines, 8(5), 129. doi:10.3390/biomedicines8050129

Guzik, T. J., Mohiddin, S. A., Dimarco, A., Patel, V., Savvatis, K., Marelli-Berg, F. M., Madhur, M. S., Tomaszewski, M., Maffia, P., D'Acquisto, F., Nicklin, S. A., Marian, A. J., Nosalski, R., Murray, E. C., Guzik, B., Berry, C., Touyz, R. M., Kreutz, R., Wang, D. W., Bhella, D., Sagliocco, O., Crea, F., Thomson, E. C., & McInnes, I. B. (2020). COVID-19 and the cardiovascular system: implications for risk assessment, diagnosis, and treatment options. Cardiovasc Res, 116(10), 1666-1687. doi:10.1093/cvr/cvaa106

Győrffy, B., Lanczky, A., Eklund, A. C., Denkert, C., Budczies, J., Li, Q., & Szallasi, Z. (2010). An online survival analysis tool to rapidly assess the effect of 22,277 genes on breast cancer prognosis using microarray data of 1,809 patients. Breast Cancer Res Treat, 123(3), 725-731. doi:10.1007/s10549-009-0674-9

Habas, K., Nganwuchu, C., Shahzad, F., Gopalan, R., Haque, M., Rahman, S., Majumder, A. A., & Nasim, T. (2020). Resolution of coronavirus disease 2019 (COVID-19). Expert Rev Anti Infect Ther, 18(12), 1201-1211. doi:10.1080/14787210.2020.1797487

Hodis, H. N., Mack, W. J., Henderson, V. W., Shoupe, D., Budoff, M. J., Hwang-Levine, J., Li, Y., Feng, M., Dustin, L., Kono, N., Stanczyk, F. Z., Selzer, R. H., & Azen, S. P. (2016). Vascular Effects of Early versus Late Postmenopausal Treatment with Estradiol. N Engl J Med, 374(13), 1221-1231. doi:10.1056/NEJMoa1505241

Hornung, V., Hartmann, R., Ablasser, A., & Hopfner, K. P. (2014). OAS proteins and cGAS: unifying concepts in sensing and responding to cytosolic nucleic acids. Nat Rev Immunol, 14(8), 521-528. doi:10.1038/nri3719

Hu, B., Guo, H., Zhou, P., & Shi, Z. L. (2021). Characteristics of SARS-CoV-2 and COVID-19. Nat Rev Microbiol, 19(3), 141-154. doi:10.1038/s41579-020-00459-7

Huang, C., Wang, Y., Li, X., Ren, L., Zhao, J., Hu, Y., Zhang, L., Fan, G., Xu, J., Gu, X., Cheng, Z., Yu, T., Xia, J., Wei, Y., Wu, W., Xie, X., Yin, W., Li, H., Liu, M., Xiao, Y., Gao, H., Guo, L., Xie, J., Wang, G., Jiang, R., Gao, Z., Jin, Q., Wang, J., & Cao, B. (2020). Clinical features of patients infected with 2019 novel coronavirus in Wuhan, China. Lancet, 395(10223), 497-506. doi:10.1016/s0140-6736(20)30183-5

Iorga, A., Umar, S., Ruffenach, G., Aryan, L., Li, J., Sharma, S., Motayagheni, N., Nadadur, R. D., Bopassa, J. C., & Eghbali, M. (2018). Estrogen rescues heart failure through estrogen receptor Beta activation. Biol Sex Differ, 9(1), 48. doi:10.1186/s13293-018-0206-6

Khan, M. S., Shahid, I., Anker, S. D., Solomon, S. D., Vardeny, O., Michos, E. D., Fonarow, G. C., & Butler, J. (2020). Cardiovascular implications of COVID-19 versus influenza infection: a review. BMC Medicine, 18(1), 403. doi:10.1186/s12916-020-01816-2

Klein, S. L., Jedlicka, A., & Pekosz, A. (2010). The Xs and Y of immune responses to viral vaccines. Lancet Infect Dis, 10(5), 338-349. doi:10.1016/s1473-3099(10)70049-9

Kotsev, S. V., Miteva, D., Krayselska, S., Shopova, M., Pishmisheva-Peleva, M., Stanilova, S. A., & Velikova, T. (2021). Hypotheses and facts for genetic factors related to severe COVID-19. World J Virol, 10(4), 137-155. doi:10.5501/wjv.v10.i4.137

Lee, J. S., Park, S., Jeong, H. W., Ahn, J. Y., Choi, S. J., Lee, H., Choi, B., Nam, S. K., Sa, M., Kwon, J. S., Jeong, S. J., Lee, H. K., Park, S. H., Park, S. H., Choi, J. Y., Kim, S. H., Jung, I., & Shin, E. C. (2020). Immunophenotyping of COVID-19 and influenza highlights the role of type I interferons in development of severe COVID-19. Sci Immunol, 5(49), eabd1554. doi:10.1126/sciimmunol.abd1554

Li, Y., Renner, D. M., Comar, C. E., Whelan, J. N., Reyes, H. M., Cardenas-Diaz, F. L., Truitt, R., Tan, L. H., Dong, B., Alysandratos, K. D., Huang, J., Palmer, J. N., Adappa, N. D., Kohanski, M. A., Kotton, D. N., Silverman, R. H., Yang, W., Morrisey, E. E., Cohen, N. A., & Weiss, S. R. (2021). SARS-CoV-2 induces double-stranded RNA-mediated innate immune responses in respiratory epithelial-derived cells and cardiomyocytes. Proc Natl Acad Sci U S A, 118(16), e2022643118. doi:10.1073/pnas.2022643118

Lu, R., Zhao, X., Li, J., Niu, P., Yang, B., Wu, H., Wang, W., Song, H., Huang, B., Zhu, N., Bi, Y., Ma, X., Zhan, F., Wang, L., Hu, T., Zhou, H., Hu, Z., Zhou, W., Zhao, L., Chen, J., Meng, Y., Wang, J., Lin, Y., Yuan, J., Xie, Z., Ma, J., Liu, W. J., Wang, D., Xu, W., Holmes, E. C., Gao, G. F., Wu, G., Chen, W., Shi, W., & Tan, W. (2020). Genomic characterisation and epidemiology of 2019 novel coronavirus: implications for virus origins and receptor binding. Lancet, 395(10224), 565-574. doi:10.1016/s0140-6736(20)30251-8

Lu, T. X., & Rothenberg, M. E. (2018). MicroRNA. J Allergy Clin Immunol, 141(4), 1202-1207. doi:10.1016/j.jaci.2017.08.034

Mapping the human genetic architecture of COVID-19. (2021). Nature, 600(7889), 472-477. doi:10.1038/s41586-021-03767-x

Mauvais-Jarvis, F., Klein, S. L., & Levin, E. R. (2020). Estradiol, Progesterone, Immunomodulation, and COVID-19 Outcomes. Endocrinology, 161(9), bqaa127. doi:10.1210/endocr/bqaa127

McMurray, J. J., & Pfeffer, M. A. (2005). Heart failure. Lancet, 365(9474), 1877-1889. doi:10.1016/s0140-6736(05)66621-4

Pairo-Castineira, E., Clohisey, S., Klaric, L., Bretherick, A. D., Rawlik, K., Pasko, D., Walker, S., Parkinson, N., Fourman, M. H., Russell, C. D., Furniss, J., Richmond, A., Gountouna, E., Wrobel, N., Harrison, D., Wang, B., Wu, Y., Meynert, A., Griffiths, F., Oosthuyzen, W., Kousathanas, A., Moutsianas, L., Yang, Z., Zhai, R., Zheng, C., Grimes, G., Beale, R., Millar, J., Shih, B., Keating, S., Zechner, M., Haley, C., Porteous, D. J., Hayward, C., Yang, J., Knight, J., Summers, C., Shankar-Hari, M., Klenerman, P., Turtle, L., Ho, A., Moore, S. C., Hinds, C., Horby, P., Nichol, A., Maslove, D., Ling, L., McAuley, D., Montgomery, H., Walsh, T., Pereira, A. C., Renieri, A., Shen, X., Ponting, C. P., Fawkes, A., Tenesa, A., Caulfield, M., Scott, R., Rowan, K., Murphy, L., Openshaw, P. J. M., Semple, M. G., Law, A., Vitart, V., Wilson, J. F., & Baillie, J. K. (2021). Genetic mechanisms of critical illness in COVID-19. Nature, 591(7848), 92-98. doi:10.1038/s41586-020-03065-y

Pasrija, R., & Naime, M. (2021). The deregulated immune reaction and cytokines release storm (CRS) in COVID-19 disease. Int Immunopharmacol, 90, 107225. doi:10.1016/j.intimp.2020.107225

Pinna, G. (2021). Sex and COVID-19: A Protective Role for Reproductive Steroids. Trends in endocrinology and metabolism: TEM, 32(1), 3-6. doi:10.1016/j.tem.2020.11.004

Ramasamy, S., & Subbian, S. (2021). Critical Determinants of Cytokine Storm and Type I Interferon Response in COVID-19 Pathogenesis. Clin Microbiol Rev, 34(3), e00299-00220. doi:10.1128/CMR.00299-20

Rebouillat, D., & Hovanessian, A. G. (1999). The human 2',5'-oligoadenylate synthetase family: interferon-induced proteins with unique enzymatic properties. J Interferon Cytokine Res, 19(4), 295-308. doi:10.1089/107999099313992

Rebouillat, D., Hovnanian, A., David, G., Hovanessian, A. G., & Williams, B. R. (2000). Characterization of the gene encoding the 100-kDa form of human 2',5' oligoadenylate synthetase. Genomics, 70(2), 232-240. doi:10.1006/geno.2000.6382

Ritchie, A. I., & Singanayagam, A. (2020). Immunosuppression for hyperinflammation in COVID-19: a double-edged sword? Lancet, 395(10230), 1111. doi:10.1016/s0140-6736(20)30691-7

Ronni, T., Matikainen, S., Sareneva, T., Melén, K., Pirhonen, J., Keskinen, P., & Julkunen, I. (1997). Regulation of IFN-alpha/beta, MxA, 2',5'-oligoadenylate synthetase, and HLA gene expression in influenza A-infected human lung epithelial cells. J Immunol, 158(5), 2363-2374.

Sabbah, H. N., & Sharov, V. G. (1998). Apoptosis in heart failure. Prog Cardiovasc Dis, 40(6), 549-562. doi:10.1016/s0033-0620(98)80003-0

Samuel, C. E. (2001). Antiviral actions of interferons. Clin Microbiol Rev, 14(4), 778-809. doi:10.1128/CMR.14.4.778-809.2001

Schwartz, S. L., & Conn, G. L. (2019). RNA regulation of the antiviral protein 2'-5'-oligoadenylate synthetase. Wiley Interdiscip Rev RNA, 10(4), e1534. doi:10.1002/wrna.1534

Schwartz, S. L., & Conn, G. L. (2019). RNA regulation of the antiviral protein 2'-5'-oligoadenylate synthetase. Wiley Interdiscip Rev RNA, 10(4), e1534-e1534. doi:10.1002/wrna.1534

Shaath, H., Vishnubalaji, R., Elkord, E., & Alajez, N. M. (2020). Single-Cell Transcriptome Analysis Highlights a Role for Neutrophils and Inflammatory Macrophages in the Pathogenesis of Severe COVID-19. Cells, 9(11), 2374. doi:10.3390/cells9112374

Shufelt, C. L., Pacheco, C., Tweet, M. S., & Miller, V. M. (2018). Sex-Specific Physiology and Cardiovascular Disease. Adv Exp Med Biol, 1065, 433-454. doi:10.1007/978-3-319-77932-4_27

Steffen, B. T., Pankow, J. S., Lutsey, P. L., Demmer, R. T., Misialek, J. R., Guan, W., Cowan, L. T., Coresh, J., Norby, F. L., & Tang, W. (2022). Proteomic profiling identifies novel proteins for genetic risk of severe COVID-19: the Atherosclerosis Risk in Communities Study. Hum Mol Genet, 31(14), 2452-2461. doi:10.1093/hmg/ddac024

Szklarczyk, D., Franceschini, A., Wyder, S., Forslund, K., Heller, D., Huerta-Cepas, J., Simonovic, M., Roth, A., Santos, A., Tsafou, K. P., Kuhn, M., Bork, P., Jensen, L. J., & von Mering, C. (2014). STRING v10: protein–protein interaction networks, integrated over the tree of life. Nucleic Acids Res, 43(D1), D447-D452. doi:10.1093/nar/gku1003

Tajbakhsh, A., Gheibi Hayat, S. M., Taghizadeh, H., Akbari, A., Inabadi, M., Savardashtaki, A., Johnston, T. P., & Sahebkar, A. (2021). COVID-19 and cardiac injury: clinical manifestations, biomarkers, mechanisms, diagnosis, treatment, and follow up. Expert Rev Anti Infect Ther, 19(3), 345-357. doi:10.1080/14787210.2020.1822737

Tavakoli, R., Nemska, S., Jamshidi, P., Gassmann, M., & Frossard, N. (2017). Technique of Minimally Invasive Transverse Aortic Constriction in Mice for Induction of Left Ventricular Hypertrophy. J Vis Exp(127), 56231. doi:10.3791/56231

van der Made, C. I., Simons, A., Schuurs-Hoeijmakers, J., van den Heuvel, G., Mantere, T., Kersten, S., van Deuren, R. C., Steehouwer, M., van Reijmersdal, S. V., Jaeger, M., Hofste, T., Astuti, G., Corominas Galbany, J., van der Schoot, V., van der Hoeven, H., Hagmolen Of Ten Have, W., Klijn, E., van den Meer, C., Fiddelaers, J., de Mast, Q., Bleeker-Rovers, C. P., Joosten, L. A. B., Yntema, H. G., Gilissen, C., Nelen, M., van der Meer, J. W. M., Brunner, H. G., Netea, M. G., van de Veerdonk, F. L., & Hoischen, A. (2020). Presence of Genetic Variants Among Young Men With Severe COVID-19. Jama, 324(7), 663-673. doi:10.1001/jama.2020.13719

Wu, C., Chen, X., Cai, Y., Xia, J., Zhou, X., Xu, S., Huang, H., Zhang, L., Zhou, X., Du, C., Zhang, Y., Song, J., Wang, S., Chao, Y., Yang, Z., Xu, J., Zhou, X., Chen, D., Xiong, W., Xu, L., Zhou, F., Jiang, J., Bai, C., Zheng, J., & Song, Y. (2020). Risk Factors Associated With Acute Respiratory Distress Syndrome and Death in Patients With Coronavirus Disease 2019 Pneumonia in Wuhan, China. JAMA Intern Med, 180(7), 934-943. doi:10.1001/jamainternmed.2020.0994

Wu, F., Zhao, S., Yu, B., Chen, Y. M., Wang, W., Song, Z. G., Hu, Y., Tao, Z. W., Tian, J. H., Pei, Y. Y., Yuan, M. L., Zhang, Y. L., Dai, F. H., Liu, Y., Wang, Q. M., Zheng, J. J., Xu, L., Holmes, E. C., & Zhang, Y. Z. (2020). A new coronavirus associated with human respiratory disease in China. Nature, 579(7798), 265-269. doi:10.1038/s41586-020-2008-3

Wu, L. F., Wang, D. P., Shen, J., Gao, L. J., Zhou, Y., Liu, Q. H., & Cao, J. M. (2022). Global profiling of protein lysine malonylation in mouse cardiac hypertrophy. J Proteomics, 266, 104667. doi:10.1016/j.jprot.2022.104667

Wu, Y., Zhang, F., Yang, K., Fang, S., Bu, D., Li, H., Sun, L., Hu, H., Gao, K., Wang, W., Zhou, X., Zhao, Y., & Chen, J. (2019). SymMap: an integrative database of traditional Chinese medicine enhanced by

symptom mapping. Nucleic Acids Res, 47(D1), D1110-D1117. doi:10.1093/nar/gky1021

Zhang, C., Feng, Y.-G., Tam, C., Wang, N., & Feng, Y. (2021). Transcriptional Profiling and Machine Learning Unveil a Concordant Biosignature of Type I Interferon-Inducible Host Response Across Nasal Swab and Pulmonary Tissue for COVID-19 Diagnosis. Front Immunol, 12, 733171-733171. doi:10.3389/fimmu.2021.733171

Zhang, C., Wu, Z., Li, J. W., Zhao, H., & Wang, G. Q. (2020). Cytokine release syndrome in severe COVID-19: interleukin-6 receptor antagonist tocilizumab may be the key to reduce mortality. Int J Antimicrob Agents, 55(5), 105954. doi:10.1016/j.ijantimicag.2020.105954

Zhou, F., Yu, T., Du, R., Fan, G., Liu, Y., Liu, Z., Xiang, J., Wang, Y., Song, B., Gu, X., Guan, L., Wei, Y., Li, H., Wu, X., Xu, J., Tu, S., Zhang, Y., Chen, H., & Cao, B. (2020). Clinical course and risk factors for mortality of adult inpatients with COVID-19 in Wuhan, China: a retrospective cohort study. Lancet, 395(10229), 1054-1062. doi:10.1016/S0140-6736(20)30566-3

Zhou, F., Yu, T., Du, R., Fan, G., Liu, Y., Liu, Z., Xiang, J., Wang, Y., Song, B., Gu, X., Guan, L., Wei, Y., Li, H., Wu, X., Xu, J., Tu, S., Zhang, Y., Chen, H., & Cao, B. (2020). Clinical course and risk factors for mortality of adult inpatients with COVID-19 in Wuhan, China: a retrospective cohort study. Lancet, 395(10229), 1054-1062. doi:10.1016/s0140-6736(20)30566-3

Zhou, Y., Zhou, B., Pache, L., Chang, M., Khodabakhshi, A. H., Tanaseichuk, O., Benner, C., & Chanda, S. K. (2019). Metascape provides a biologist-oriented resource for the analysis of systems-level datasets. Nat Commun, 10(1), 1523. doi:10.1038/s41467-019-09234-6

Zhou, Z., Ren, L., Zhang, L., Zhong, J., Xiao, Y., Jia, Z., Guo, L., Yang, J., Wang, C., Jiang, S., Yang, D., Zhang, G., Li, H., Chen, F., Xu, Y., Chen, M., Gao, Z., Yang, J., Dong, J., Liu, B., Zhang, X., Wang, W., He, K., Jin, Q., Li, M., & Wang, J. (2020). Heightened Innate Immune Responses in the Respiratory Tract of COVID-19 Patients. Cell Host Microbe, 27(6), 883-890. doi:10.1016/j.chom.2020.04.017

Figure legends

Figure 1. Data processing and hub genes screening in GSE150392. (**A**) Volcano plot of DEGs from GSE150392. X-axis indicates log2(FC) and the Y-axis indicates -log10(P-value). Red and green dot represent upregulated and downregulated DEGs, respectively. grey dot represents indifference genes. (**B**) Heatmap of all genes, each column represents sample, colors of green to red in each row represent the expression level of gene. (**C**) OAS gene family expression in GSE150392. (**D**) PPI network of DEGs were showed with dots, red dot is hub genes as showed in E. (**E**) Top 30 hub genes calculated by cytohubba. In these genes, OAS1, OAS2, OAS3, and OASL rank is 14,13,9, and 28, respectively.

Figure 2. Data processing and hub genes screening in GSE120852. (**A**) Volcano plot of DEGs from GSE120852. X-axis indicates log2(FC) and the Y-axis indicates -log10(P-value). Red and green dot represent upregulated and downregulated DEGs, respectively. grey dot represents indifference genes. Result of diff1and diff3 come from left ventricle (LV)tissue, result of diff2 and diff4 come from right ventricle (RV) tissue, diff1 and diff2 is the result of comparing the left ventricle heart failure (LV-HF) and (NF) heart. diff3 and diff4 is the result of comparing the biventricular heart failure (Bi-HF) and NF heart. (**B**) Heatmap of all genes, each column represents sample, colors of green to red in each row represents the expression level of gene. RV-NF: right ventricle tissue, not failure heart; LV-NF: left ventricle tissue, not failure heart; RV-HF: right ventricle tissue, heart failure; RV-Bi-HF: right ventricle tissue, biventricular heart failure; LV-HF: left ventricle tissue, heart failure; LV-Bi-HF: left ventricle tissue, heart failure. (**C**) Venn diagram of DEGs in GSE120862. There are 239 common different gene in diff1- 4, 169 were up-expressed and 70 were down-expressed. (**D**) OAS gene family expression in GSE120862. (**E**) PPI network of common DEGs were showed with dots. Yellow dot is hub genes showed as F. (**F**) Top 30 hub genes calculated by cytohubba. In these genes, OAS1, OAS2, OAS3, and OASL rank is 15,2,6, and 6, respectively.

Figure 3. Experimental verification the expression of OAS gene family in SARS-CoV-2 infected NHBE and

COVID-19 blood. (**A**) OAS1, OAS2, OAS3, and OASL expression in GSE147507, NHBE: Mock treated primary human lung epithelium NHBE cells, n=3; SARS-CoV-2 infected NHBE, n=3. (**B**) OAS1, OAS2, OAS3, and OASL expression in GSE179850, Healthy control, n=16; COVID-19 patient, n=31. *P<0.05, **P<0.01, ***P<0.001.

Figure 4. Experimental verification the expression of OAS gene family in HF. (**A**) Representative heart sizes from each group (left of upper) and M-mode echocardiography of heart (right of upper), measurement of HW/BW, EF%, FS%, LVPWD, and LVPWS (bottom row), (n = 4). (**B**) qPCR analysis of ANP, BNP, β-MHC, OAS1, OAS2, OAS3 and OASL mRNA levels in sham and 8W TAC heart. The data are normalized to the GAPDH expression (n = 4). ANP, BNP, and β-MHC is heart failure markers. (**C**) H9C2 treated with PBS and Ang II (1 μM) for 48 hours and performed to determine cell size with phalloidin and DAPI. (**D**) qPCR analysis of ANP, BNP, β-MHC, OAS1, OAS2, OAS3 and OASL mRNA levels in PBS and 1 μM Ang II treated H9C2. The data are normalized to the GAPDH expression (n = 4). ANP, BNP, and β-MHC is heart failure markers, *P<0.05, **P<0.01, ***P<0.001.

Figure 5. GO and KEGG pathway enrichment analysis of DEGs in GSE150392 by Metascape. (**A**) GO enrichment analysis. (**B**) KEGG pathway enrichment analysis.

Figure 6. GO and KEGG pathway enrichment analysis of common DEGs in GSE120852 by Metascape. (**A**) GO enrichment analysis. (**B**) KEGG pathway enrichment analysis.

Figure 7. miRNAs that regulate OAS gene family. (**A**) Volcano plot (left) and heatmap (right) of different expressed miRNAs in GSE104150. (**B**) Common miRNAs come from the intersection of GSE105150 and Targetscan database.

Figure 8. Chemical or ingredient that interacted with OAS gene family from CTD and SymMap database. (**A**) Chemicals interacted with OAS gene family. There are 12, 14, 10, and 6 chemicals interact with OAS1, OAS2, OAS3, and OASL, respectively. Red circle means OAS gene family, yellow triangle means chemical, blue triangle means common chemical. (**B**) Ingredients that reacted with OAS gene family. There are 4, 3, 5, and 4 ingredients act on OAS1, OAS2, OAS3, and OASL, respectively. Red circle means OAS gene family, green diamond means drug, orange diamond means common ingredient.

Figure 9. Docking analysis of affinity between chemicals/ingredients and OAS1 (**A**), OAS2 (**B**), OAS3 (**C**), and OASL (**D**).

Figure 10. The mechanism of OAS genes and the process of causing HF after cardiomyocytes are infected with SARS-CoV-2.

Table 1. Detail information of GSE150392

GEO accession	Organism	Platform	Contributor(s)	Samples
GSE150392	Homo sapiens (Cell)	GPL18573	Sharma A, et al	SARS-CoV-2 Infected hiPSC- cardiomyocytes 3

Table 2. Detail information of GSE120852

GEO accession	Organism	Platform	Contributor(s)	Contributor(s)	Samples	Samples	Samples	Samples	Samples	Samples	Samples	S
GSE120852	Homo sapiens (Heart tissue)	GPL11154	Luo X, et al		Diff-1	Diff-1	Diff-2	Diff-2	Diff-3	Diff-3	I	

Condition	Condition	Non Failing (NF)	Left Ventricle Heart Failure (LV-HF)	Non Failing (NF)	Left Ventricle Heart Failure (LV-HF)	Non Failing (NF)	BiVentricul Heart Failure (Bi-HF)	H
Tissue	Tissue	Left Ventricle (LV) 5	Left Ventricle (LV) 5	Right Ventricle (RV) 5	Right Ventricle (RV) 5	Left Ventricle (LV) 5	Left Ventricle (LV) 5	L V (5

Table 3. Detail information of GSE147507

GEO accession	Organism	Platform	Contributor(s)	Samples	Samples
GSE147507	Homo sapiens (Cell)	GPL18573	Sharma A, et al	Mock treated NHBE cells 3	NHBE infected with 3

Table 4. Detail information of GSE179850

GEO accession	Organism	Platform	Contributor(s)	Samples	Samples
GSE179850	Homo sapiens (Blood)	GPL28038	Ebihara T, et al	Healthy control 16	COVID-19 patient 31

Table 5. Detail information of GSE104150 (microRNA expression dataset)

GEO accession	Organism	Platform	Contributor(s)	Samples	Samples
GSE104150	Homo sapiens (Blood)	GPL20712	Liu W, et al	Healthy control 7	Heart failure 9

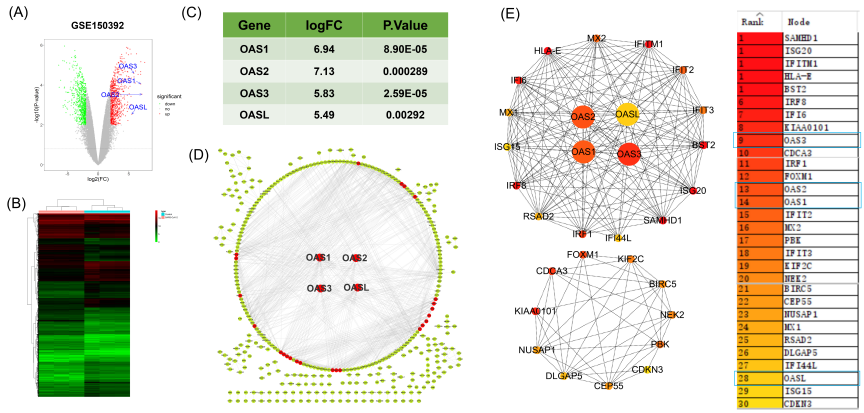

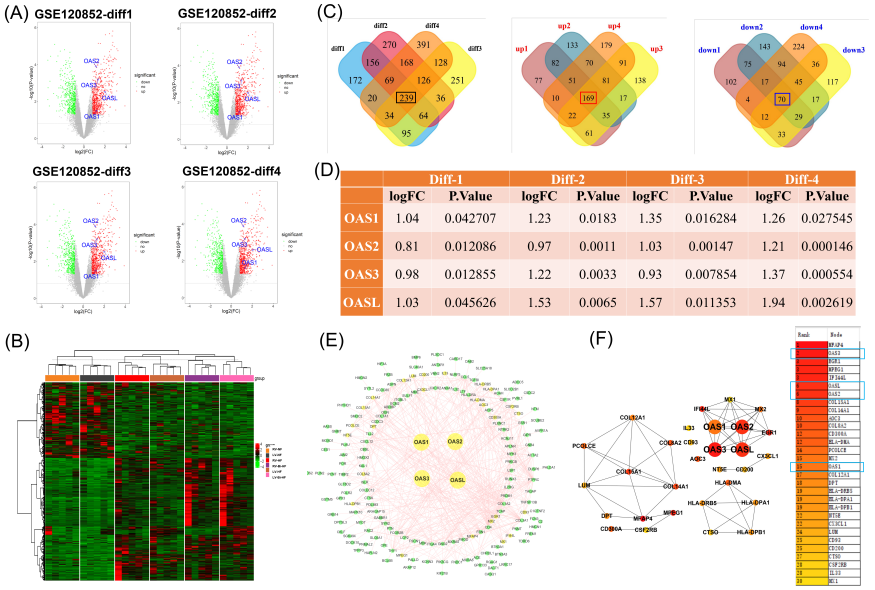

(D)

	Diff-1		Diff-2		Diff-3		Diff-4	
	logFC	P.Value	logFC	P.Value	logFC	P.Value	logFC	P.Value
OAS1	1.04	0.042707	1.23	0.0183	1.35	0.016284	1.26	0.027545
OAS2	0.81	0.012086	0.97	0.0011	1.03	0.00147	1.21	0.000146
OAS3	0.98	0.012855	1.22	0.0033	0.93	0.007854	1.37	0.000554
OASL	1.03	0.045626	1.53	0.0065	1.57	0.011353	1.94	0.002619